

The Fundamental Fuzzy Logic Operators and some Complex Boolean Logic Circuits Implemented by the Chromogenism of a Spirooxazine.

Pier Luigi Gentili*

Dipartimento di Chimica, Università di Perugia, 06123 Perugia (Italy)

pierluigi.gentili@unipg.it

ELECTRONIC SUPPLEMENTARY INFORMATION

Photochromism

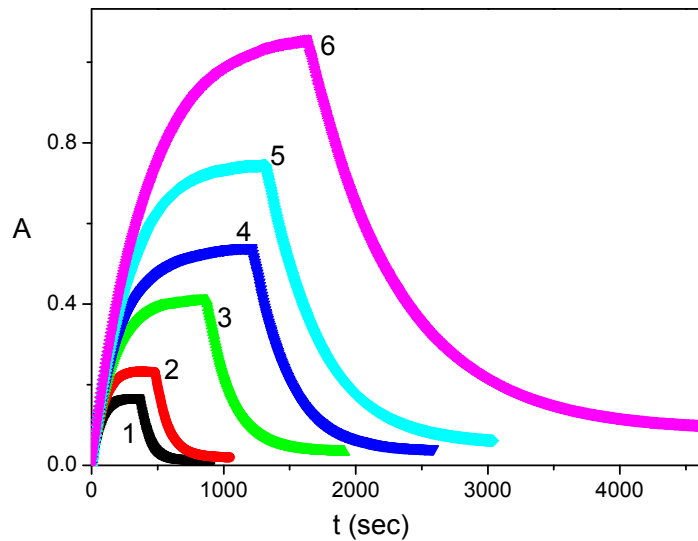


Figure S.1. Kinetics of photo-colouration and bleaching recorded at 611 nm and at different temperatures: (1) 298 K, (2) 295 K, (3) 290 K, (4) 287.5 K, (5) 285 K, (6) 280 K. The irradiation of SpO was carried out at 379 nm and the intensity was of the order of 10^7 moles of quanta $\text{dm}^{-3}\text{s}^{-1}$. The conversion degree of SpO to MC are 5% at 298 K and 34% at 280 K for a SpO's solution having an analytical concentration of 3.2×10^{-5} M.

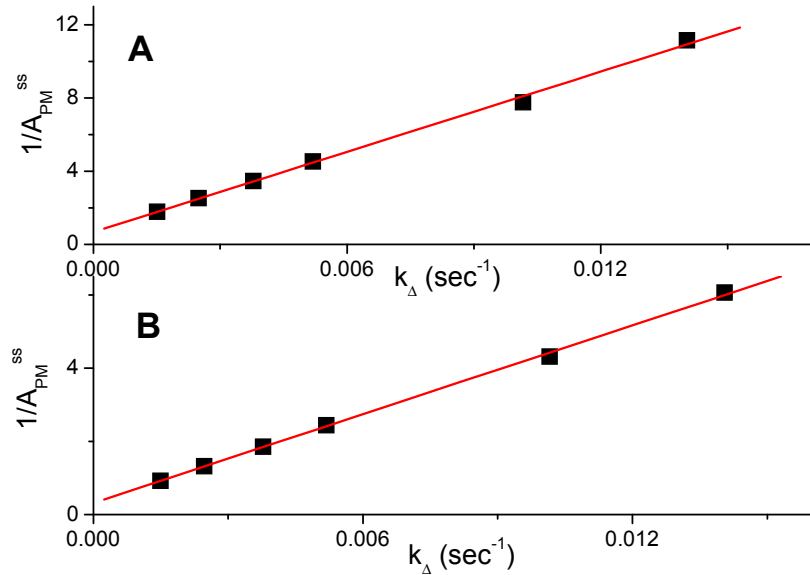


Figure S.2. Treatment of the kinetic data, A_{MC}^{∞} and k_{Δ} , according to equation (6) of the paper. The points of graph (A) are relative to $\lambda_{an}=580$ nm; they are fitted by a straight line (red trace) having an intercept $A=(0.68\pm 0.14)$, a slope $B=(729.9\pm 18.7)$ and a correlation coefficient $r=0.99869$. The points in graph (B) are relative to $\lambda_{an}=611$ nm; they are fitted by a straight line having an intercept $A=(0.318\pm 0.046)$, a slope $B=(403.9\pm 6.1)$ and a correlation coefficient $r=0.99955$.

Acidichromism

The photochemical transformation describing the acidichromism of SpO is (1s):



The differential kinetic equation describing the spectral evolution due to the photochemical transformation (1s) is:

$$\frac{dA_{\text{H}^+ - \text{MC}}}{dt} = \epsilon_{\text{H}^+ - \text{MC}} l \Phi_{\text{H}^+ - \text{MC}} I_{\text{SpO}} \quad (2\text{s})$$

wherein $A_{\text{H}^+ - \text{MC}}$ and $\epsilon_{\text{H}^+ - \text{MC}}$ are the absorbance and the molar absorption coefficient of $\text{H}^+ - \text{MC}$, respectively; $\Phi_{\text{H}^+ - \text{MC}}$ is the photo-reaction quantum yield; l is the optical path length and I_{SpO} is the intensity of the radiation absorbed by SpO. Just in the first steps of the chemical transformation, the content of the product can be overlooked. Therefore, equation (2s) can be approximated by the equation (3s), below:

$$\frac{dA_{H^+-MC}}{dt} = \epsilon_{H^+-MC} l \Phi_{H^+-MC} I_0 (1 - 10^{-A'_{SpO}(t=0)}) \quad (3s)$$

wherein $A'_{SpO}(t=0)$ is the absorbance of SpO at the irradiation wavelength, before starting to irradiate. The value of Φ_{H^+-MC} can be determined by using the initial velocity method and equation (3s), if ϵ_{H^+-MC} is already known. In case of a prolonged irradiation, equation (3s) is not valid anymore, since I'_{SpO} has to be expressed by equation (4s):

$$I'_{SpO} = \frac{A'_{SpO}}{A'_{TOT}} (1 - 10^{-A'_{TOT}}) I'_0 = A'_{SpO} F I'_0 \quad (4s)$$

wherein A'_{SpO} and A'_{TOT} are the absorbance values of SpO alone, and SpO along with H^+-MC , respectively, at the irradiation wavelength (λ_{irr}) and F represents the photo-kinetic factor. F is constant if λ_{irr} corresponds to the wavelength of an isosbestic point. Introducing equation (4s) into equation (2s), we obtain equation (5s):

$$\frac{dA_{H^+-MC}}{dt} = \epsilon_{H^+-MC} l \Phi_{H^+-MC} I'_0 F A'_{SpO} = \epsilon_{H^+-MC} l \Phi_{H^+-MC} I'_0 F \epsilon'_{SpO} l \left(C_0 - \frac{A_{H^+-MC}}{\epsilon_{H^+-MC}} \right) \quad (5s)$$

By separating the variables and integrating between $[0,t]$ and $[A_{H^+-MC}(t=0), A_{H^+-MC}(t)]$, equation (6s) is achieved:

$$A_{H^+-MC}(t) = \epsilon_{H^+-MC} l C_0 - (\epsilon_{H^+-MC} l C_0 - A_{H^+-MC}(t=0)) e^{-\Phi_{H^+-MC} F I'_0 \epsilon'_{SpO} l t} \quad (6s)$$

It becomes equation (8) of the paper when $A_{H^+-MC}(t=0)=0$.

By applying equation (6s), it results that $\Phi_{H^+-MC} = (0.25 \pm 0.01)$ and $\epsilon_{H^+-MC} (485 \text{ nm}) = (17600 \pm 250) \text{ M}^{-1} \text{ cm}^{-1}$ for $\lambda_{irr}=320 \text{ nm}$. The value of Φ_{H^+-MC} for $\lambda_{irr}=379 \text{ nm}$, determined through the initial velocity method and equation (3s), is equal to that evaluated for $\lambda_{irr}=320 \text{ nm}$.

Metallochromism

To determine the quantum yield of the photoreaction producing $\text{Al}^{3+}\text{-MC}$ and the molar absorption coefficient of the complex, the following procedure was used. The value of the absorbance at the maximum of the colour band (i.e. at 485 nm), recorded at the photo-stationary state (see Figure 3 of the full paper), is $A_{TOT}^\infty (485\text{nm}) = 0.413$. The contribution of $H^+\text{-MC}$ to $A^\infty (485\text{nm})$ amounts to 9%, as stated into the paper. Therefore, it is possible to estimate the concentration of $H^+\text{-MC}$ at the photo-stationary state:

$$[\text{H}^+ - \text{MC}]^\infty = \frac{0.09(A_{\text{TOT}}^\infty(485\text{nm}))}{\epsilon_{\text{H}^+ - \text{MC}}} \quad (7s)$$

Since the photo-reaction has been carried out at low temperature, where the thermal process of bleaching is negligible, the concentration of Al^{3+} -MC can be determined by the difference (8s), assuming a complete conversion of SpO into the two coloured products:

$$[\text{Al}^{3+} - \text{MC}]^\infty = C_0 - [\text{H}^+ - \text{MC}]^\infty \quad (8s).$$

When $[\text{Al}^{3+} - \text{MC}]^\infty$ is known, it is possible to determine $\epsilon_{\text{Al}^{3+} - \text{MC}}$ and $\Phi_{\text{Al}^{3+} - \text{MC}}$ through the equations (9s) and (10s), respectively:

$$\epsilon_{\text{Al}^{3+} - \text{MC}} = \frac{A_{\text{TOT}}^\infty(485\text{nm})(1 - 0.09)}{[\text{Al}^{3+} - \text{MC}]^\infty} \quad (9s)$$

$$\Phi_{\text{Al}^{3+} - \text{MC}} = \frac{[\text{Al}^{3+} - \text{MC}]^\infty}{I'_0 \Delta t (1 - 10^{-A_{\text{TOT}}^\infty})} \quad (10s)$$

wherein I'_0 is the intensity of the irradiation source, A_{TOT}^∞ is the total absorbance at the isosbestic point, and Δt is the time interval of irradiation.

(1) Spectra recorded at the photo-stationary states in the presence of HClO_4 and $\text{Cu}(\text{ClO}_4)_2$:

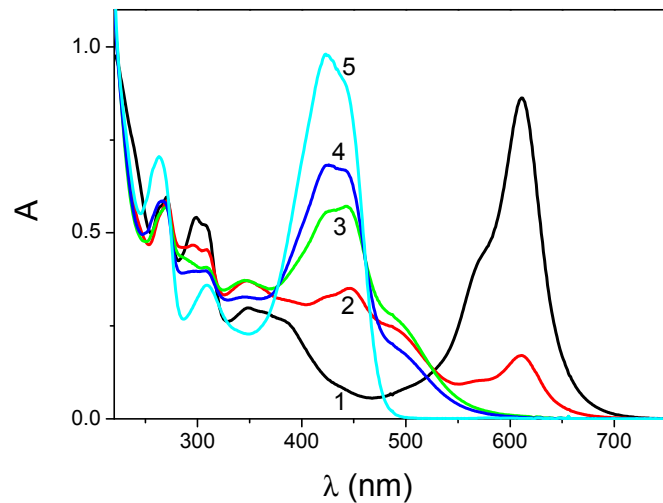


Figure S.3. Absorption spectra recorded at the photo-stationary state for different molar ratios of HClO_4 to SpO ($n_{\text{H}^+}/n_{\text{SpO}} = r_1$) and $\text{Cu}(\text{ClO}_4)_2$ to SpO ($n_{\text{Cu}^{2+}}/n_{\text{SpO}} = r_2$). Spectra: 1 (black) for $r_1=0$, $r_2=0$; 2 (red) for $r_1=0.33$, $r_2=0.33$; 3 (green) for $r_1=0.33$, $r_2=0.66$; 4 (blue) for $r_1=0.33$, $r_2=1$; 5 (cyan) for $r_1=0.33$, $r_2=1.5$.

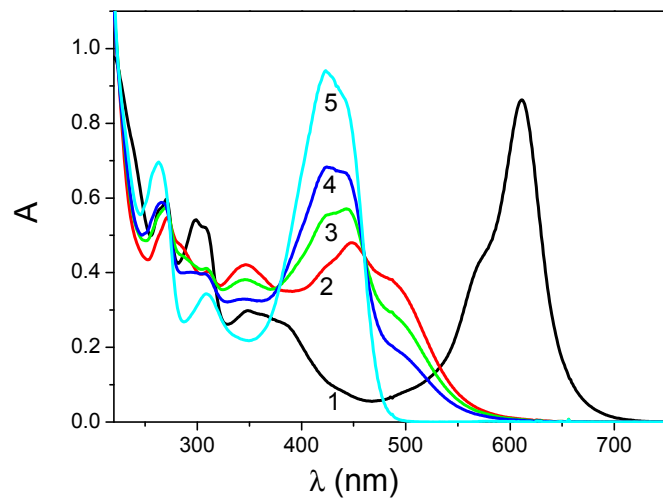


Figure S.4. Absorption spectra recorded at the photo-stationary state for different molar ratios of HClO_4 to SpO ($n_{\text{H}^+}/n_{\text{SpO}} = r_1$) and $\text{Cu}(\text{ClO}_4)_2$ to SpO ($n_{\text{Cu}^{2+}}/n_{\text{SpO}} = r_2$). Spectra: 1 (black) for $r_1=0$, $r_2=0$; 2 (red) for $r_1=0.66$, $r_2=0.33$; 3 (green) for $r_1=0.66$, $r_2=0.66$; 4 (blue) for $r_1=0.66$, $r_2=1$; 5 (cyan) for $r_1=0.66$, $r_2=1.5$.

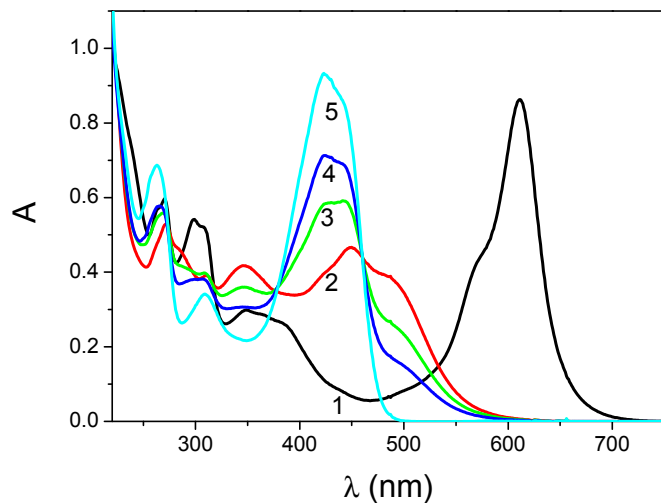


Figure S.5. Absorption spectra recorded at the photo-stationary state for different molar ratios of HClO_4 to SpO ($n_{\text{H}^+}/n_{\text{SpO}} = r_1$) and $\text{Cu}(\text{ClO}_4)_2$ to SpO ($n_{\text{Cu}^{2+}}/n_{\text{SpO}} = r_2$). Spectra: 1 (black) for $r_1=0$, $r_2=0$; 2 (red) for $r_1=1$, $r_2=0.33$; 3 (green) for $r_1=1$, $r_2=0.66$; 4 (blue) for $r_1=1$, $r_2=1$; 5 (cyan) for $r_1=1$, $r_2=1.5$.

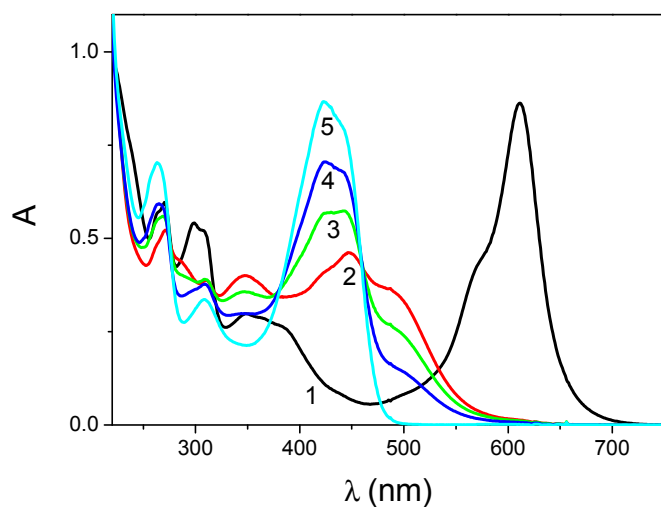


Figure S.6. Absorption spectra recorded at the photo-stationary state for different molar ratios of HClO_4 to SpO ($n_{\text{H}^+}/n_{\text{SpO}} = r_1$) and $\text{Cu}(\text{ClO}_4)_2$ to SpO ($n_{\text{Cu}^{2+}}/n_{\text{SpO}} = r_2$). Spectra: 1 (black) for $r_1=0$, $r_2=0$; 2 (red) for $r_1=1.5$, $r_2=0.33$; 3 (green) for $r_1=1.5$, $r_2=0.66$; 4 (blue) for $r_1=1.5$, $r_2=1$; 5 (cyan) for $r_1=1.5$, $r_2=1.5$.

(2) Spectra recorded at the photo-stationary states in the presence of $HClO_4$ and $AlCl_3$:

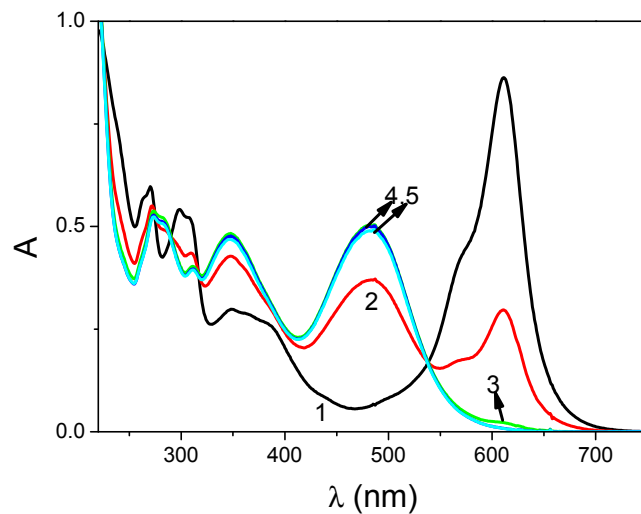


Figure S.7. Absorption spectra recorded at the photo-stationary state for different molar ratios of $HClO_4$ to SpO ($n_{H^+} / n_{SpO} = r_1$) and $AlCl_3$ to SpO ($n_{Al^{3+}} / n_{SpO} = r_3$). Spectra: 1 (black) for $r_1=0$, $r_3=0$; 2 (red) for $r_1=0.33$, $r_3=0.18$; 3 (green) for $r_1=0.33$, $r_3=0.33$; 4 (blue) for $r_1=0.33$, $r_3=0.67$; 5 (cyan) for $r_1=0.33$, $r_3=1$.

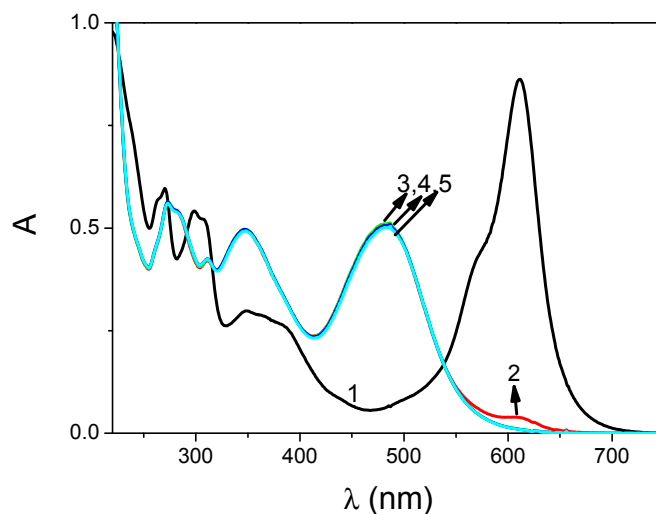


Figure S.8. Absorption spectra recorded at the photo-stationary state for different molar ratios of $HClO_4$ to SpO ($n_{H^+} / n_{SpO} = r_1$) and $AlCl_3$ to SpO ($n_{Al^{3+}} / n_{SpO} = r_3$). Spectra: 1 (black) for $r_1=0$, $r_3=0$; 2 (red) for $r_1=0.7$, $r_3=0.18$; 3 (green) for $r_1=0.7$, $r_3=0.35$; 4 (blue) for $r_1=0.7$, $r_3=0.65$; 5 (cyan) for $r_1=0.7$, $r_3=1$.

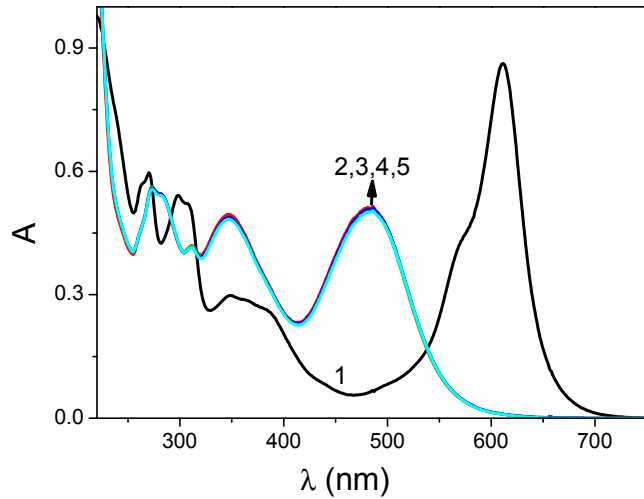


Figure S.9. Absorption spectra recorded at the photo-stationary state for different molar ratios of HClO_4 to SpO ($n_{\text{H}^+}/n_{\text{SpO}} = r_1$) and AlCl_3 to SpO ($n_{\text{Al}^{3+}}/n_{\text{SpO}} = r_3$). Spectra: 1 (black) for $r_1=0$, $r_3=0$; 2 (red) for $r_1=1$, $r_3=0.18$; 3 (green) for $r_1=1$, $r_3=0.35$; 4 (blue) for $r_1=1$, $r_3=0.65$; 5 (cyan) for $r_1=1$, $r_3=1$.

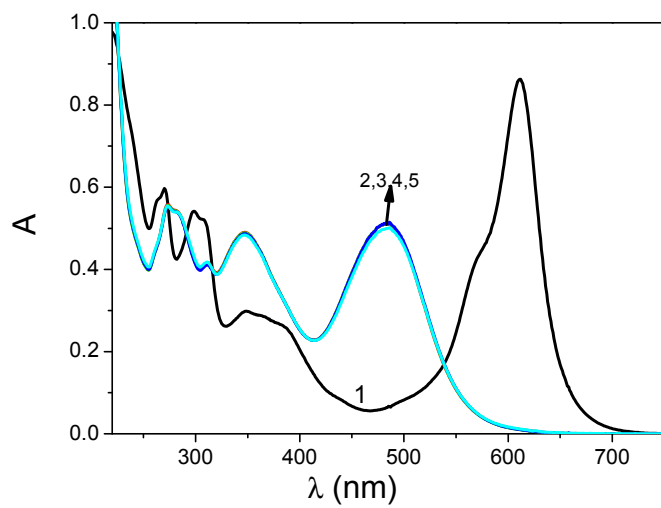


Figure S.10. Absorption spectra recorded at the photo-stationary state for different molar ratios of HClO_4 to SpO ($n_{\text{H}^+}/n_{\text{SpO}} = r_1$) and AlCl_3 to SpO ($n_{\text{Al}^{3+}}/n_{\text{SpO}} = r_3$). Spectra: 1 (black) for $r_1=0$, $r_3=0$; 2 (red) for $r_1=1.6$, $r_3=0.18$; 3 (green) for $r_1=1.6$, $r_3=0.35$; 4 (blue) for $r_1=1.6$, $r_3=0.65$; 5 (cyan) for $r_1=1.6$, $r_3=1$.

(3) Spectra recorded at the photo-stationary states in the presence of AlCl_3 and $\text{Cu}(\text{ClO}_4)_2$:

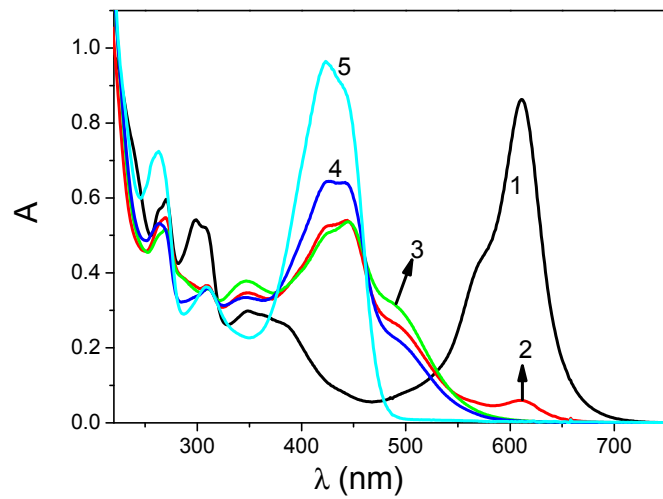


Figure S.11. Absorption spectra recorded at the photo-stationary state for different molar ratios of AlCl_3 to SpO ($n_{\text{Al}^{3+}} / n_{\text{SpO}} = r_3$) and $\text{Cu}(\text{ClO}_4)_2$ to SpO ($n_{\text{Cu}^{2+}} / n_{\text{SpO}} = r_2$). Spectra: 1 (black) for $r_3=0$, $r_2=0$; 2 (red) for $r_3=0.33$, $r_2=0.33$; 3 (green) for $r_3=0.33$, $r_2=0.66$; 4 (blue) for $r_3=0.33$, $r_2=1$; 5 (cyan) for $r_3=0.33$, $r_2=1.5$.

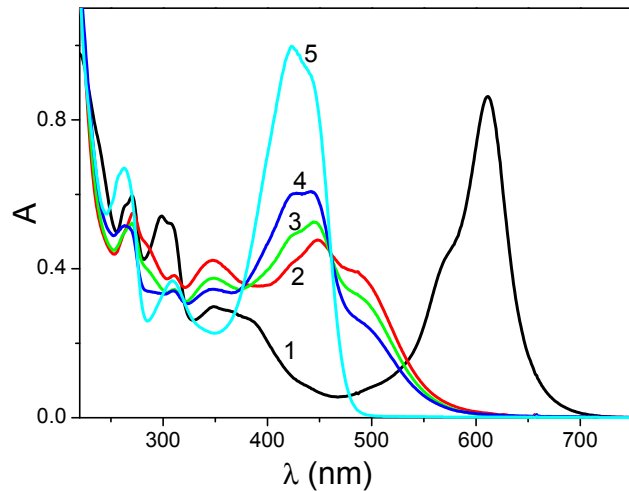


Figure S.12. Absorption spectra recorded at the photo-stationary state for different molar ratios of AlCl_3 to SpO ($n_{\text{Al}^{3+}} / n_{\text{SpO}} = r_3$) and $\text{Cu}(\text{ClO}_4)_2$ to SpO ($n_{\text{Cu}^{2+}} / n_{\text{SpO}} = r_2$). Spectra: 1 (black) for $r_3=0$, $r_2=0$; 2 (red) for $r_3=0.66$, $r_2=0.33$; 3 (green) for $r_3=0.66$, $r_2=0.66$; 4 (blue) for $r_3=0.66$, $r_2=1$; 5 (cyan) for $r_3=0.66$, $r_2=1.5$.

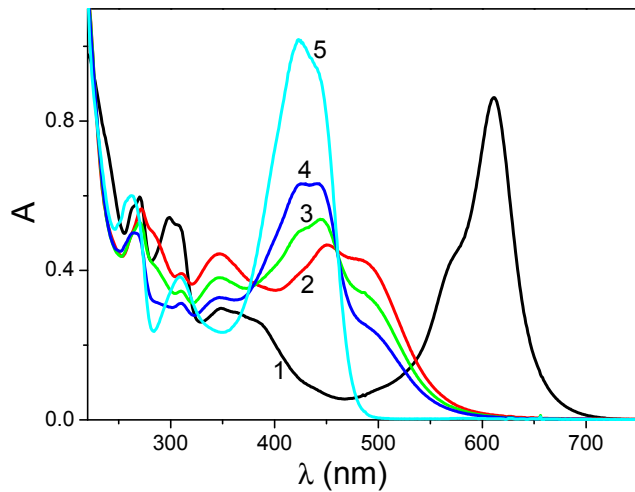


Figure S.13. Absorption spectra recorded at the photo-stationary state for different molar ratios of AlCl_3 to SpO ($n_{\text{Al}^{3+}} / n_{\text{SpO}} = r_3$) and $\text{Cu}(\text{ClO}_4)_2$ to SpO ($n_{\text{Cu}^{2+}} / n_{\text{SpO}} = r_2$). Spectra: 1 (black) for $r_3=0$, $r_2=0$; 2 (red) for $r_3=1$, $r_2=0.33$; 3 (green) for $r_3=1$, $r_2=0.66$; 4 (blue) for $r_3=1$, $r_2=1$; 5 (cyan) for $r_3=1$, $r_2=1.5$.

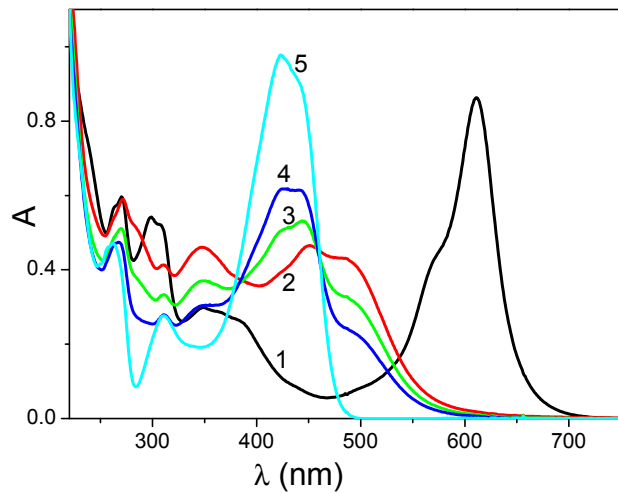


Figure S.14. Absorption spectra recorded at the photo-stationary state for different molar ratios of AlCl_3 to SpO ($n_{\text{Al}^{3+}} / n_{\text{SpO}} = r_3$) and $\text{Cu}(\text{ClO}_4)_2$ to SpO ($n_{\text{Cu}^{2+}} / n_{\text{SpO}} = r_2$). Spectra: 1 (black) for $r_3=0$, $r_2=0$; 2 (red) for $r_3=1.5$, $r_2=0.33$; 3 (green) for $r_3=1.5$, $r_2=0.66$; 4 (blue) for $r_3=1.5$, $r_2=1$; 5 (cyan) for $r_3=1.5$, $r_2=1.5$.

Table S1. Values of the tristimulus variables X, Y, Z and the RGB colour coordinates as function of the n_{H^+}/n_{SpO} and $n_{Al^{3+}}/n_{SpO}$ molar ratios.

n_{H^+}/n_{SpO}	$n_{Al^{3+}}/n_{SpO}$	X	Y	Z	R	G	B
0	0	0.4324	0.5487	0.8977	28.1	165	220
0.33	0	0.4351	0.5268	0.7358	59.5	152	177
0.7	0	0.5574	0.5952	0.5759	154	153	132
1	0	0.7746	0.7226	0.4473	255	159	94.0
1.5	0	0.7761	0.7213	0.4507	255	158	95.0
0	0.18	0.4358	0.5167	0.6998	68.7	147	168
0	0.35	0.5746	0.5911	0.5396	175	146	123
0	0.65	0.7552	0.7035	0.4554	255	155	96.9
0	1	0.7656	0.7099	0.4420	255	155	93.1
0	1.5	0.7721	0.7173	0.4463	255	157	94.0
0.33	0.18	0.5884	0.6108	0.5503	177	153	125
0.33	0.33	0.7651	0.7142	0.4532	255	157	95.9
0.33	0.66	0.7795	0.7255	0.4570	255	159	96.5
0.33	1	0.7813	0.7286	0.4627	255	160	97.9
0.7	0.18	0.7497	0.7048	0.4467	255	157	94.4
0.7	0.35	0.7748	0.7215	0.4458	255	158	93.6
0.7	0.65	0.7756	0.7216	0.4495	255	158	94.6
0.7	1	0.7770	0.7225	0.4553	255	158	96.2
1	0.18	0.7765	0.7227	0.4478	255	159	94.2
1	0.35	0.7774	0.7233	0.4560	255	159	96.3
1	0.65	0.7751	0.7192	0.4527	255	157	95.6
1	1	0.7777	0.7216	0.4591	255	158	97.3
1.6	0.18	0.7755	0.7205	0.4520	255	158	95.4
1.6	0.35	0.7758	0.7198	0.4523	255	157	95.5
1.6	0.65	0.7750	0.7178	0.4530	255	157	95.8
1.6	1	0.7747	0.7190	0.4607	255	157	97.8

Table S2. Values of the tristimulus variables X, Y, Z and the RGB colour coordinates as function of the n_{H^+} / n_{SpO} , $n_{Cu^{2+}} / n_{SpO}$ molar ratios.

n_{H^+} / n_{SpO}	$n_{Cu^{2+}} / n_{SpO}$	X	Y	Z	R	G	B
0	0	0.4324	0.5487	0.8977	28.1	165	220
0.33	0	0.4351	0.5268	0.7358	59.5	152	177
0.7	0	0.5574	0.5952	0.5759	154	153	132
1	0	0.7746	0.7226	0.4473	255	159	94.0
1.5	0	0.7761	0.7213	0.4507	255	158	95.0
0	0.33	0.5245	0.6473	0.6516	96.9	187	149
0	0.67	0.65684	0.75616	0.45321	189	204	92.2
0	1	0.7536	0.8204	0.3810	253	210	70.7
0	1.5	0.8115	0.9571	0.3692	248	255	61.3
0.33	0.33	0.6777	0.7297	0.5276	207	187	114
0.33	0.66	0.7857	0.8162	0.3804	255	200	71.2
0.33	1	0.7932	0.8548	0.3680	255	217	66.0
0.33	1.5	0.8142	0.9618	0.3762	248	255	62.9
0.67	0.33	0.7798	0.7722	0.4010	255	181	79.0
0.67	0.66	0.7836	0.8087	0.3758	255	197	70.4
0.67	1	0.7915	0.8513	0.3669	255	216	65.9
0.67	1.5	0.8165	0.9631	0.3878	248	255	66.0
1	0.33	0.7823	0.7702	0.4092	255	179	81.3
1	0.66	0.7879	0.8219	0.3758	255	202	69.7
1	1	0.7969	0.8680	0.3708	255	222	66.1
1	1.5	0.8182	0.9653	0.3909	248	255	66.8
1.5	0.33	0.7757	0.7670	0.4159	255	180	83.2
1.5	0.66	0.7803	0.8107	0.3841	255	199	72.4
1.5	1	0.7944	0.8679	0.3807	255	223	68.8
1.5	1.5	0.8205	0.9639	0.4114	248	255	72.4

Table S3. Values of the tristimulus variables X, Y, Z and the RGB colour coordinates as function of the $n_{Al^{3+}}/n_{SpO}$, $n_{Cu^{2+}}/n_{SpO}$ molar ratios.

$n_{Al^{3+}}/n_{SpO}$	$n_{Cu^{2+}}/n_{SpO}$	X	Y	Z	R	G	B
0	0	0.4324	0.5487	0.8977	28.1	165	220
0.18	0	0.4358	0.5167	0.6998	68.7	147	168
0.35	0	0.5746	0.5911	0.5396	175	146	123
0.65	0	0.7552	0.7035	0.4554	255	155	96.9
1	0	0.7656	0.7099	0.4420	255	155	93.1
1.5	0	0.7721	0.7173	0.4463	255	157	94.0
0	0.33	0.5245	0.6473	0.6516	96.9	187	149
0	0.67	0.65684	0.75616	0.45321	189	204	92.2
0	1	0.7536	0.8204	0.3810	253	210	70.7
0	1.5	0.8115	0.9571	0.3692	248	255	61.3
0.33	0.33	0.7398	0.7785	0.3998	255	194	77.8
0.33	0.66	0.7835	0.7959	0.3845	255	191	73.4
0.33	1	0.7892	0.8364	0.3663	255	209	66.4
0.33	1.5	0.8098	0.9525	0.3771	248	255	63.6
0.66	0.33	0.7712	0.7582	0.4005	255	176	79.5
0.66	0.66	0.78109	0.7889	0.3877	255	188	74.6
0.66	1	0.7799	0.8142	0.3689	255	201	68.2
0.66	1.5	0.8120	0.9586	0.3708	248	255	61.6
1	0.33	0.7657	0.7414	0.3994	255	170	80.0
1	0.66	0.7753	0.7826	0.3793	255	187	72.5
1	1	0.7811	0.8200	0.3618	255	203	66.0
1	1.5	0.8096	0.9575	0.3672	247	255	60.7
1.5	0.33	0.7562	0.7291	0.3990	255	166	80.4
1.5	0.66	0.7747	0.7819	0.3863	255	187	74.5
1.5	1	0.7867	0.8261	0.3768	255	205	69.8
1.5	1.5	0.8168	0.9663	0.3808	248	255	64.0

Rules for the Fuzzy Logic System FLS_1 having H^+ and Al^{3+} as inputs

When the action of the chemical inputs H^+ and Al^{3+} are combined, a FLS based upon the rules' matrix shown in Table 5 of the main paper can be implemented.

The rules are the following statements:

- (1) IF n_{H^+}/n_{SpO} AND $n_{Al^{3+}}/n_{SpO}$ are null, THEN the colour is Blue;
- (2) IF n_{H^+}/n_{SpO} is low OR $n_{Al^{3+}}/n_{SpO}$ is low, THEN the colour is Blue-Green, i.e. cyan;
- (3) IF n_{H^+}/n_{SpO} is medium OR $n_{Al^{3+}}/n_{SpO}$ is medium, THEN the solution is Red-Green-Blue, i.e. grey;
- (4) IF n_{H^+}/n_{SpO} is high OR $n_{Al^{3+}}/n_{SpO}$ is high, THEN the solution is Red;
- (5) IF n_{H^+}/n_{SpO} is very high OR $n_{Al^{3+}}/n_{SpO}$ is very high, THEN the solution is Red;
- (6) IF n_{H^+}/n_{SpO} is low AND $n_{Al^{3+}}/n_{SpO}$ is low, THEN the solution is Red-Green, i.e. yellow;
- (7) IF n_{H^+}/n_{SpO} is low AND $n_{Al^{3+}}/n_{SpO}$ is NOT low, THEN the solution is Red;
- (8) IF $n_{Al^{3+}}/n_{SpO}$ is low AND n_{H^+}/n_{SpO} is NOT low, THEN the solution is Red;
- (9) IF $n_{Al^{3+}}/n_{SpO}$ is medium AND n_{H^+}/n_{SpO} is NOT low, THEN the solution is Red;
- (10) IF $n_{Al^{3+}}/n_{SpO}$ is high AND n_{H^+}/n_{SpO} is NOT low, THEN the solution is Red;
- (11) IF $n_{Al^{3+}}/n_{SpO}$ is very high AND n_{H^+}/n_{SpO} is NOT low, THEN the solution is Red.

Rules for the Fuzzy Logic System FLS_2 having H^+ and Cu^{2+} as inputs

In the case of the chemical inputs H^+ and Cu^{2+} , a new FLS can be implemented, whose rules' matrix is shown in Table 6 of the paper.

The rules are the following statements:

- (1) IF n_{H^+}/n_{SpO} AND $n_{Cu^{2+}}/n_{SpO}$ are null, THEN the solution is Blue;
- (2) IF $n_{Cu^{2+}}/n_{SpO}$ is low AND n_{H^+}/n_{SpO} is null, THEN the solution is Green;
- (3) IF $n_{Cu^{2+}}/n_{SpO}$ is medium AND n_{H^+}/n_{SpO} is null, THEN the solution is Green-Red, i.e. yellow;
- (4) IF $n_{Cu^{2+}}/n_{SpO}$ is high AND n_{H^+}/n_{SpO} is null, THEN the solution is Red-Green, i.e. yellow;
- (5) IF $n_{Cu^{2+}}/n_{SpO}$ is very high, THEN the solution is Green-Red, i.e. yellow;
- (6) IF n_{H^+}/n_{SpO} is low AND $n_{Cu^{2+}}/n_{SpO}$ is null, THEN the solution is Blue-Green, i.e. cyan;
- (7) IF n_{H^+}/n_{SpO} is medium AND $n_{Cu^{2+}}/n_{SpO}$ is null, THEN the solution is Red-Green-Blue i.e. grey;
- (8) IF n_{H^+}/n_{SpO} is high AND $n_{Cu^{2+}}/n_{SpO}$ is null, THEN the solution is Red;
- (9) IF n_{H^+}/n_{SpO} is very high AND $n_{Cu^{2+}}/n_{SpO}$ is null, THEN the solution is Red;
- (10) IF n_{H^+}/n_{SpO} is low AND $n_{Cu^{2+}}/n_{SpO}$ is low, THEN the solution is Red-Green, i.e. yellow;
- (11) IF n_{H^+}/n_{SpO} is medium AND $n_{Cu^{2+}}/n_{SpO}$ is NOT vey high, THEN the solution is Red;
- (12) IF n_{H^+}/n_{SpO} is high AND $n_{Cu^{2+}}/n_{SpO}$ is NOT vey high, THEN the solution is Red;
- (13) IF n_{H^+}/n_{SpO} is very high AND $n_{Cu^{2+}}/n_{SpO}$ is NOT vey high, THEN the solution is Red;
- (14) IF n_{H^+}/n_{SpO} is low AND $n_{Cu^{2+}}/n_{SpO}$ is medium, THEN the solution is Red;
- (15) IF n_{H^+}/n_{SpO} is low AND $n_{Cu^{2+}}/n_{SpO}$ is high, THEN the solution is Red.